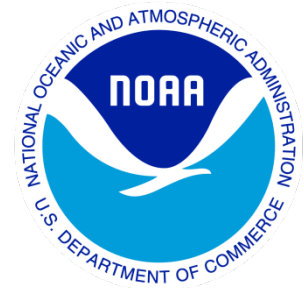

Climate Data Record (CDR) Program

Climate Algorithm Theoretical Basis Document (C-ATBD)

NOAA's NEXRAD Reanalysis

C-ATBD: Precipitation – NEXRAD QPE CDR



CDR Program Document Number: CDRP-ATBD-0917

Configuration Item Number: 01B-22

Revision 0 / August 3, 2017

REVISION HISTORY

Rev.	Author	DSR No.	Description	Date
0	Brian Nelson NOAA/NESDIS/NCEI	DSR- 1163	Initial Submission to CDR Program	08/03/2017

TABLE of CONTENTS

1. INTRODUCTION.....	6
1.1 Purpose	6
1.2 Definitions	6
1.3 Referencing this Document.....	7
1.4 Document Maintenance	8
2. OBSERVING SYSTEMS OVERVIEW.....	9
2.1 Products Generated	10
2.2 Instrument Characteristics	11
3. ALGORITHM DESCRIPTION.....	13
3.1 Algorithm Overview	13
3.2 Processing Outline	13
3.2.1 Reading Input.....	13
3.2.2 Geolocation Correction.....	14
3.2.3 Quality Control.....	14
3.2.4 Calculating Reflectivity.....	14
3.2.5 Precipitation Type Classification	15
3.2.6 Radar Only Precipitation Rates	16
3.2.7 Gauge Correction Quantitative Precipitation Estimates.....	16
3.2.8 Writing Output.....	17
3.3 Algorithm Input	17
3.3.1 Primary Sensor Data	17
3.3.2 Ancillary Data.....	17
3.3.3 Derived Data	18
3.3.4 Forward Models.....	18
3.4 Theoretical Description	18
3.4.1 Physical and Mathematical Description.....	18
3.4.2 Data Merging Strategy	19
3.4.3 Numerical Strategy	19
3.4.4 Calculations.....	19
3.4.5 Look-Up Table Description.....	19
3.4.6 Parameterization	19
3.4.7 Algorithm Output.....	19
4. TEST DATASETS AND OUTPUTS.....	20
4.1 Test Input Datasets	20
4.2 Test Output Analysis	20
4.2.1 Reproducibility	20
4.2.2 Precision and Accuracy	20
4.2.3 Error Budget.....	20

5. PRACTICAL CONSIDERATIONS..... 21

5.1 Numerical Computation Considerations 21

5.2 Programming and Procedural Considerations 21

5.3 Quality Assessment and Diagnostics..... 21

5.4 Exception Handling 21

 5.4.1 Conditions Checked21

 5.4.2 Conditions Not Checked22

 5.4.3 Conditions Not Considered Exceptions.....22

5.5 Algorithm Validation..... 22

 5.5.1 Geolocation Correction.....22

 5.5.2 Scan Bias Correction22

5.6 Processing Environment and Resources 22

6. ASSUMPTIONS AND LIMITATIONS 23

6.1 Algorithm Performance 23

6.2 Sensor Performance..... 23

7. FUTURE ENHANCEMENTS..... 24

7.1 Enhancement 1 – Backfill of NEXRAD-Re Record..... 24

7.2 Enhancement 2 – Extension of the NEXRAD-Re Record..... 24

8. REFERENCES..... 25

APPENDIX A. ACRONYMS AND ABBREVIATIONS 28

APPENDIX B. NEXRAD DETAILS 29

LIST of FIGURES

Figure 1: CONUS-wide NEXRAD coverage. Range rings are 230km. Radar overlap areas are shown in shaded areas. 9

Figure 2: NEXRAD vertical scan. R is range (km), Theta (degrees) gate..... 11

Figure 3: NEXRAD doppler pulse. D is distance to target at time T1. D+A is distance to target at time T2. 12

Figure 4: Overall processing flow chart 15

LIST of TABLES

Table 1: NEXRAD Reanalysis QPE product attributes 10

Table 2: Precipitation Type Identifiers..... 15

Table 3: Error Budget of NEXRAD Reanalysis..... 20

1. Introduction

1.1 Purpose

The purpose of this document is to describe the algorithm submitted to the National Centers for Environmental Information (NCEI-NC) by Brian Nelson, Principal Investigator from the NOAA/NESDIS/NCEI, that will be used to create the NOAA NEXRAD Reanalysis. The actual algorithm is defined by the computer program (code) that accompanies this document, and thus the intent here is to provide a guide to understanding that algorithm, from both a scientific perspective and in order to assist a software engineer or end-user performing an evaluation of the code.

NOAA's NEXRAD reanalysis consists of two primary components; (1) Severe weather and radar-reflectivity data generation, (2) Quantitative Precipitation Estimate (including associated precipitation variables and merged rain gauge and radar estimation). This document focuses on the second component of NOAA's NEXRAD reanalysis – the Quantitative Precipitation Estimate (QPE).

1.2 Definitions

Marshall Palmer Z-R relationship (Marshall and Palmer, 1948):

$$R=(Z/a)^{1/b} \quad (1)$$

where a and b are constants and,

R= rain rate in mm/hr

Z= radar reflectivity (dB)

Radar Quality Index (RQI) (Zhang et al. 2012)

$$RQI = RQI_{blk} \cdot RQI_{hgt} \quad (2)$$

$$RQI_{blk} = \begin{cases} 1; & blk \leq 10\% \\ \left(1 - \frac{blk-0.1}{0.4}\right); & 10\% < blk < 50\% \\ 0; & blk > 50\% \end{cases}$$

$$RQI_{hgt} = \begin{cases} 1; & h_{0C} > D_{bb} \cap h_a < h_{0C} - D_{bb} \\ \vdots \\ \exp\left(-\frac{(h_a - h_{0C} + D_{bb})^2}{H^2}\right); & h_{0C} > D_{bb} \cap h_a \geq h_{0C} - D_{bb} \\ \vdots \\ \exp\left[-\frac{h_a^2}{H^2}\right]; & h_{0C} \leq D_{bb} \end{cases}$$

RQI_{blk} : RQI based on blockages; RQI_{hgt} : RQI based on radar beam height; h_a : height of beam axis (m above radar level [m ARL]); h_{0C} : height of 0° C (m ARL); D_{bb} : depth of bright band layer (m); blk : beam blockages (dimensionless); H : a height scale factor (m)

Hybrid Scan Reflectivity

(3)

$$HSR = \frac{\sum_i w_L^i \times w_H^i \times SHSR^i}{\sum_i w_L^i \times w_H^i}$$

$$w_L = \exp\frac{d^2}{L^2}$$

$$w_H = \exp-\frac{h^2}{H^2}$$

HSR represents the mosaicked hybrid scan reflectivity, i is the radar index and $SHSR$ is the single radar hybrid scan reflectivity field. The horizontal weighting field is w_L and the vertical weighting field is w_H . The variable d represents the distance between analysis point and the radar, and h represents the height of the single radar HSR bin. L and H are the scale factors of the two weighting functions.

1.3 Referencing this Document

This document should be referenced as follows:

NEXRAD QPE - Climate Algorithm Theoretical Basis Document, NOAA Climate Data Record Program CDRP-ATBD-0917 Rev 0 (2017). Available at <http://www.ncdc.noaa.gov/cdr/atmospheric>

1.4 Document Maintenance

Synchronization between this document and the algorithm is achieved through version and revision numbers, i.e., there will be consistency between the version numbers on the front cover of this document and the version and revision numbers contained within the software itself (i.e., various header files within the software documentation).

2. Observing Systems Overview

This section provides an overview of the characteristics of the NEXRAD observing systems and its calibration strategy. For more specific details on NEXRAD sensors, please refer to Appendix B and references.

The NEXRAD network is based on 144 Weather Surveillance Radar – 1988 Doppler (WSR-88D) pedestals. NEXRAD sites operate at S band and have a clear air and precipitation scanning strategy. In addition there are 3 eras. The first is the legacy era with data generated at 1 degree and 1 km gate range. The second is the high resolution that is operated at 0.5 degrees and 100 m gate range, and the third is the dual-polarization era that operates at the high resolution but adds additional moments K_{dp} and Φ_{dp} . Several authors describe the NEXRAD network. See Klazura and Imy (1993), Crum et al. (1993), and Cunha et al. (2013).

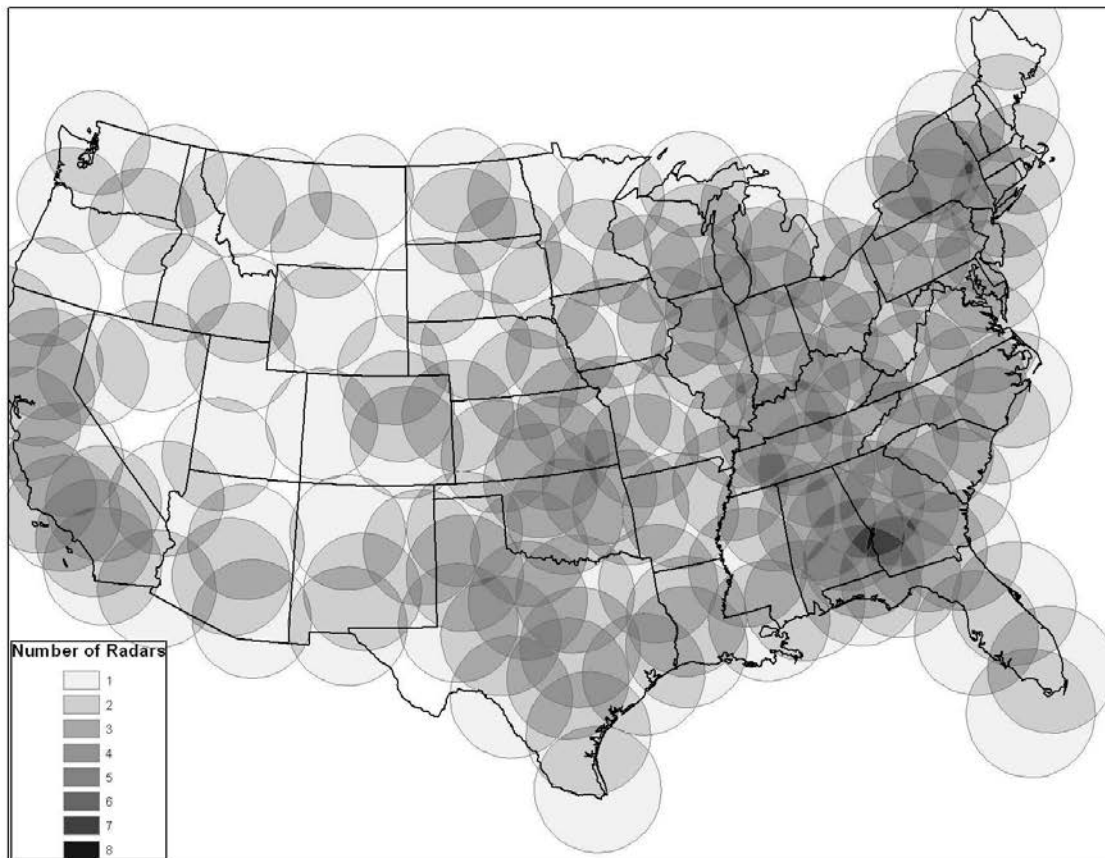


Figure 1: CONUS-wide NEXRAD coverage. Range rings are 230km. Radar overlap areas are shown in shaded areas.

2.1 Products Generated

The primary data sets generated from this algorithm are radar-only and radar-gauge merged precipitation products as well as ancillary information on precipitation type and radar quality. Further details are provided in Table 1. The initial data set covers the time period from January 2002 – December 2011. The data are stored in netCDF version 4.0 files that include the necessary metadata and supplementary data fields which are described in detail in Section 3.4.7 (see submission agreement).

Table 1: NEXRAD Reanalysis QPE product attributes

ID	Unit	Temporal resolution	Description
MOS2D	dBZ	5-minute	Two-dimensional gridded reflectivity
RQIND	dimensionless	5-minute	Radar Quality Indicator
PFLAG	dimensionless	5-minute	Precipitation Flag
PRATE	mm/hr	5-minute	Precipitation rate (uncorrected)
ROQPE	Mm/hr	1-hour	Radar-only Quantitative Precipitation Estimate

GCQPE	Mm/hr	1-hour	Gauge Corrected Quantitative Precipitation Estimate
-------	-------	--------	---

2.2 Instrument Characteristics

NEXRAD is an S-band (10 cm) polar scanning ground based microwave sensor that scans 17 levels in the atmosphere (Figure 2) (Battan 1973). Its primary function is to track storms through wind and precipitation measurement. It does this by translating the reflected radar pulse into 3 moments – reflectivity, Doppler radial velocity and width of the Doppler velocity spectrum (Battan 1973). The reflectivity can be translated into rainfall via the well know relations between drop size distribution and reflectivity and then rainfall is converted via the well known reflectivity to rainfall relations (Marshall and Palmer, 1948).

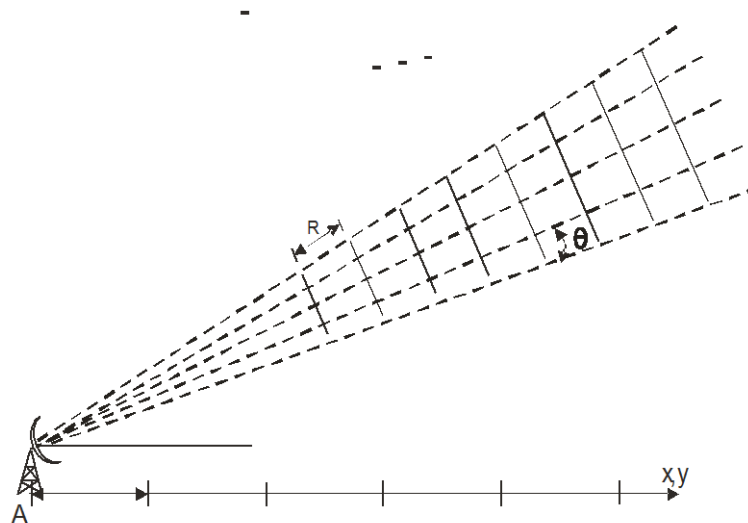


Figure 2: NEXRAD vertical scan. R is range (km), Theta (degrees) gate.

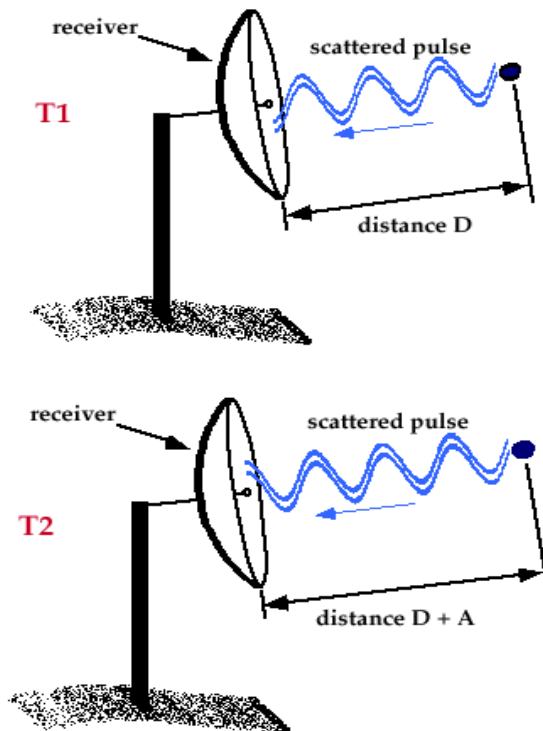


Figure 3: NEXRAD doppler pulse. D is distance to target at time T1. D+A is distance to target at time T2.

3. Algorithm Description

3.1 Algorithm Overview

This section describes the generation of NEXRAD Reanalysis QPE products described in Table 1. It provides an overview of the inter-radar calibration, geolocation, the mosaicing of single radars, the quality processing of radar data, and the merging of radar data to composite reflectivity. In addition this section provide details on the conversion of the composite reflectivity to precipitation which generates the NEXRAD Reanalysis QPE products.

The details of the inter-radar calibration, geolocation, the mosaicing of single radars, the quality processing of radar data, and the merging of radar data to composite reflectivity can be found in Lakshmanan et al. 2007. In that publication (Lakshmanan et al. 2007) Figures 1 and 2 provide the data flow for parts 1 and parts 2 of the WDSS-II processing algorithm. Part 1 of WDSS-II is a system to create 2D and 3D products at 1-km resolution over the continental U.S. The first level of applications are data ingest applications. The other applications provide meteorological products derived from a single source (Lakshmanan et al. 2007). Part 2 of the data flow shows the creation of 3D and dervied 2D products that cover the entire spatial domain (Lakshmanan et al. 2007).

The details of the QPE processing algorithm (previously named NMQ or National Mosaic and Multi-sensor QPE system) can be found in Zhang et al. 2011. Figure 1 in Zhang et al. 2011 provides the overarching flow chart of the NMQ system. This flowchart includes the generation of radar quality control, 3D mosaicing of radar, quantitative precipitaiton estimation and the resulting products that arise from this process.

3.2 Processing Outline

The steps of the NEXRAD reanalysis algorithms include reading the input data (Level II), processing the data via WDSS-II, writing the severe and reflectivity data, generating precipitation products via the NMQ, and merging radar-only precipitation data and rain gauge data and the writing of the output data (FCDR). The overall processing flow is shown in Figure 4.

3.2.1 Reading Input

WDSS-II is the algorithm that reads the data and generates the severe weather and reflectivity data. The first level of applications in WDSS-II (Fig 1 in Lakshmanan et al. 2007) are the ingest applications (ldm2netcdf and ltgingest). Essentially WDSS-II reads all the level II data for all available radars for the specified time step. WDSS-II runs applications on the level II data for steps like hail diagnosis, vertically integrated liquid, shear velocity, and quality control of reflectivity data. These processes are referred to as the severe weather applications. After reading and quality control of the level II data WDSS-II assembles the reflectivity data into 2-dimensional and 3-dimensional grids on the conus-wide scale. At this point the NMQ system reads the reflectivity inputs to produce the QPE (Zhang et al 2011).

3.2.2 Geolocation Correction

WDSS-II does the processing of the NEXRAD level II data from its native format polar format (Zhang et al 2011) to 3-D Cartesian grid centered at the radar site in a cylindrical equidistant map projection. Zhang et al 2011 provide the details for the single radar Cartesian grid. Single radar 3D reflectivity Cartesian grids from multiple radars are combined into a 3D reflectivity mosaic grid that covers the CONUS and parts of Canada. The mosaic domain spans 130° to 60° W longitude and 20° to 55° N latitude. The grid is on the cylindrical equidistant map projection and has a resolution of 0.01° x 0.01°. The resolution in the east-west direction is approximately 1.045 km at the southern bound and 0.638 km at the northern bound. The resolution in the north-south direction is approximately 1.112 km everywhere.

3.2.3 Quality Control

Weather radar data are subject to many contaminants, mainly due to non-precipitating targets such as insects and wind-borne particles, anomalous propagation, and ground clutter. Automated weather algorithms have difficulty identifying these contaminants. Lakshmanan et al. 2007 provide the overview of the quality control neural network (QCNN) that is used to automatically identify contaminants in the single radar reflectivity data. Knowledge of the surface temperature at the radar site is useful for distinguishing between summertime bloom and wintertime snow, so that information is extracted from model analysis grids and presented to the quality control neural network (Lakshmanan et al. 2005).

Weather radar are also subject to quality issues related to beam blockage and the vertical profile of reflectivity (VPR). Zhang et al. 2012 provide a detailed overview of the radar quality indicator (RQI). The RQI is a dimensionless index that combines a measure for beam blockage and vertical profile of reflectivity effects on a CONUS scale. This measure is mainly aimed at the radar QPE uncertainty associated with (1) VPR and (2) beam blockage. The equation is thus a function of the RQI due to VPR and RQI due to beam blockage. Equation 2 from section 1.2 provides RQI_{blk} and RQI_{hgt} and then the RQI as a function of both. An advantage of RQI is that it is generated every 5-minutes and each radar precipitation rate field has an associated RQI field.

Rain gauge data are used in the correction of radar data as described in section 3.2.8. The rain gauge data used in the NOAA NEXRAD reanalysis

3.2.4 Calculating Reflectivity

The radar based Q2 is computed from the hybrid scan reflectivity (HSR). Single radar HSR fields are mosaicked to product a regional HSR field. The HSR mosaic scheme and associated weighting functions are defined in section 1.2 (Zhang et al 2011).

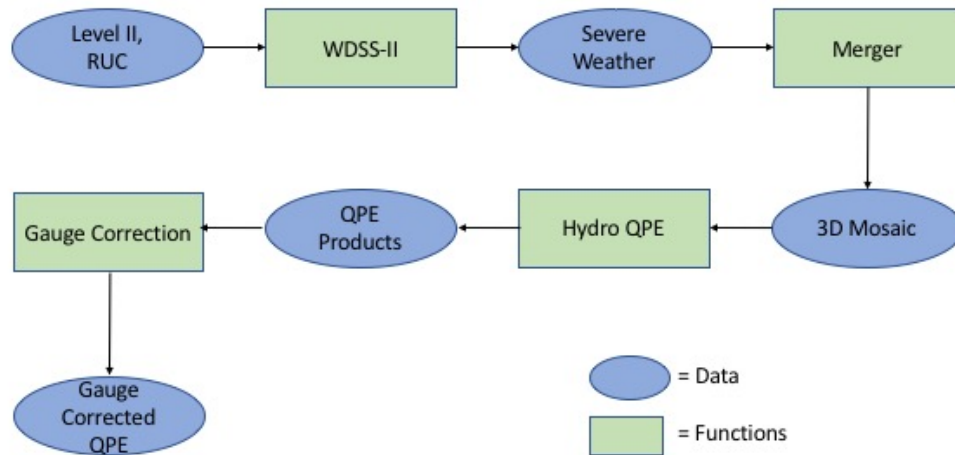


Figure 4: Overall processing flow chart

3.2.5 Precipitation Type Classification

Zhang et al 2011 provide the details for generating the precipitation type variable. Multiple precipitation regimes often coexist within a single radar site. The NMQ provides an automated precipitation classification based on the 3D radar reflectivity structure and atmospheric environmental data. The NMQ classification of precipitation regimes consists of a series of physically based heuristic rules (see Zhang et al 2011). Each grid point is assigned a precipitation type based on 3D reflectivity structure and the environmental thermal and moisture fields. Table 2 shows the precipitation types identified in the PFLAG variable.

Table 2: Precipitation Type Identifiers

Value	Precipitation Type
-1	Missing
0	No Precipitation
1	Stratiform/Warm Stratiform
2	Brightband
3	Snow

4	Overshooting
6	Convective
7	Hail
9	Warm Rain
10	Tropical Stratiform
91	Tropical Convective
96	Cool Stratiform

3.2.6 Radar Only Precipitation Rates

The NMQ radar-only precipitation rates are obtained by applying Z-R relationships to the mosaicked HSR field pixel by pixel. Zhang et al 2011 provide the overview of precipitation rate generation. Four Z-R relationships are used in association with the precipitation type field.

Convective (Fulton et al. 1998) $Z=300R^{1.4}$ (4)

Stratiform (Marshall et al. 1955) $Z=200R^{1.6}$ (5)

Warm Rain (Rosenfeld et al. 1993) $Z=230R^{1.25}$ (6)

Snow at surface (R.O.C. 1999) $Z=75R^{2.0}$ (7)

Z represents radar reflectivity (mm^6/m^3) and R represents rain rate or snow water equivalent (mm/hr). The convective Z-R is capped at 55dBZ for convective rain. It is also applied to hail pixels with a cap of 49 dBZ. A cap is also applied to the warm-rain Z-R relationships (see Zhang et al 2011). The precipitation rate field is calculated every 2.5 min. The 1-hour accumulations are computed every 5-minutes by aggregating the rate fields.

3.2.7 Gauge Correction Quantitative Precipitation Estimates

Bias correction of radar QPEs in the NMQ system is based on an additive radar rainfall error model. The details can be found in Zhang et al. 2011. The first step is to calculate an additive radar-rainfall error at each rain gauge location according to

$$e_i = r_i - g_i \quad (8)$$

where e is the error at the i th rain gauge, r is the radar-estimated rainfall and g is the gauge-observed rainfall measurement. Error values are then interpolated over the predefined radar domain using

$$R = \frac{\sum_i e_i w_i}{\sum_i w_i} \quad (9)$$

Where R is the estimated radar error at the pixel being interpolated, w is the weight assigned to the ith rain gauge and n represents the total number of matching gauge and radar pairs.

The method used to calculate the weights is a modified version of inverse distance weighting (IDW) found in Simanton and Osborn (1980). Zhang et al. 2011 provide the details on the weighting scheme applied to the radar-rainfall and rain gauge estimates.

3.2.8 Writing Output

The calculation results and meta information are written out in NetCDF4 format. Information such as conventions, title, and product version etc. is recorded in the attribute fields. In the data fields, variables are divided into two groups: data, and geolocation and time. In the data group, the recorded variables are mosaicked 2-dimensional reflectivity, precipitation rate, precipitation flag, radar quality indicator, radar-only quantitative precipitation estimate, and gauge corrected quantitative precipitation estimate. Data in the geolocation and time group include latitude, longitude, and observation time.

3.3 Algorithm Input

3.3.1 Primary Sensor Data

The Next Generation Weather Radar (NEXRAD) system currently comprises 160 sites throughout the United States and select overseas locations. Although the NOAA NEXRAD Reanalysis only uses data from the 143 CONUS NEXRAD sites. The NCEI archive includes the base data, called Level-II, and the derived products, called Level-III. Level-II data include the original three meteorological base data quantities: reflectivity, mean radial velocity, and spectrum width, as well as the dual-polarization base data of differential reflectivity, correlation coefficient, and differential phase. The NOAA NEXRAD reanalysis used the Level II data as inputs to the processing algorithm (Figure 4). All NEXRAD Level-II data are available through NCEI. Data collection and recording are in the unit of files, which typically contain four, five, six, or ten minutes of base data depending on the volume coverage pattern.

Through cooperative activities as a part of NOAA's Big Data Project (BDP), NEXRAD data are now freely available through the following cloud infrastructures. NCEI releases the NOAA NEXRAD archive inventory as a reference for users in support of the BDP efforts. The inventory contains comma separated (CSV) text files listing the original archive files (in tar format) and the individual volume scans present inside the tar files. Example scripts showing how to automate the listing, access and conversion files are available (<https://www1.ncdc.noaa.gov/pub/data/radar/bdp/scripts/>).

3.3.2 Ancillary Data

Rapid Update Cycle

The production package requires the Rapid Update Cycle (RUC) data. The Rapid Update Cycle (RUC) is an operational atmospheric prediction system comprised primarily of a numerical forecast model and an analysis system to initialize that model. The RUC has been developed to serve users needing short-range weather forecasts. RUC runs operationally at the National Centers for Environmental Prediction (NCEP). Data have been obtained through the Department of Energy Atmospheric Radiation Measurement Climate Research Facility (DOE-ARM) (<https://dis.arm.gov/instruments/ruc>).

Hydrometeorological Automated Data System (HADS)

The Hydrometeorological Automated Data System (HADS) is a real-time data acquisition and data distribution system operated by the National Weather Service Office of Dissemination. (<https://hads.ncep.noaa.gov/>).

Community Collaborative Hail, Rain, Hail, and Snow Network

CoCoRaHS is an acronym for the Community Collaborative Rain, Hail and Snow Network. CoCoRaHS is a unique, non-profit, community-based network of volunteers of all ages and backgrounds working together to measure and map precipitation (rain, hail and snow). By using low-cost measurement tools, stressing training and education, and utilizing an interactive Web-site, our aim is to provide the highest quality data for natural resource, education and research applications.

Climate Reference Network

The U.S. Climate Reference Network (USCRN) is a systematic and sustained network of climate monitoring stations with sites across the conterminous U.S., Alaska, and Hawaii. These stations use high-quality instruments to measure temperature, precipitation, wind speed, soil conditions, and more. Information is available on what is measured and the USCRN station instruments (<https://www.ncdc.noaa.gov/crn/>).

3.3.3 Derived Data

The operational system does not require any derived data.

3.3.4 Forward Models

Not applicable.

3.4 Theoretical Description

3.4.1 Physical and Mathematical Description

3.4.1.1 Geolocation Correction

NEXRAD does not have a Geolocation Correction. Georeferencing takes place at the NEXRAD site and then the conversion of data from polar to cartesian coordinates takes place in merging of the site specific level II data as described in section 3.2.2. The technical

memorandum (Fulton 1998) provides detail on the conversion of NEXRAD polar data to a cartesian coordinate system.

3.4.1.2 Inter-Satellite Calibration

Not Applicable

3.4.1.3 Scan Bias Correction

Not Applicable

3.4.2 Data Merging Strategy

WDSS-II includes several tools for remapping, rescaling, transforming coordinate systems and combining data from multiple sensors and placing them onto a common earth-relative, constantly updating grid.

3.4.3 Numerical Strategy

3.4.4 Calculations

Details on the processing steps involved in the algorithm are provided in Section 3.2.

3.4.5 Look-Up Table Description

Not applicable.

3.4.6 Parameterization

Parameterization for the conversion of reflectivity to precipitation is based on the defined precipitation type. Section 3.2.6 shows the four Z-R precipitation conversions used in the NOAA NEXRAD reanalysis.

3.4.7 Algorithm Output

Table 1 provides the details of the 6 variables included in the NOAA NEXRAD reanalysis. The MOS2D variable is provided at 5-minute resolution at 1x1 km². The PRATE variable is provided at 5-minute resolution at 1x1 km². The RQIND variable is provided at 5-minute resolution at 1x1 km². The PFLAG variable is provided at 5-minute resolution at 1x1 km². The ROQPE and GCQPE variables are provided at hourly resolution at 1x1 km².

4. Test Datasets and Outputs

4.1 Test Input Datasets

Not applicable

4.2 Test Output Analysis

4.2.1 Reproducibility

Running the processing codes to the input datasets, users should recover same results except for rounding errors.

4.2.2 Precision and Accuracy

The quality of data depends on instrument health. The NEXRAD sensor status is recorded and provided online by NCEI at <https://www.ncdc.noaa.gov/nexradinv/> and at NWS Radar Operations Center <https://www.roc.noaa.gov/WSR88D/>.

4.2.3 Error Budget

The various errors associated with the NEXRAD processing are listed in Table 3. It is noted that these errors cannot be combined in simple forms.

Table 3: Error Budget of NEXRAD Reanalysis

Error Sources	Magnitude of Errors	Algorithm improvement
<i>Non-precipitating targets (insects, birds, anomalous propagation, and ground clutter)</i>	<i>unknown</i>	<i>Neural Network (Lakshmanan et al 2005)</i>
<i>Beam Blockage and Vertical Profile of Reflectivity</i>	<i>1-100 (dependant on magnitude of blockage)</i>	<i>Radar Quality Indicator (Zhang et al. 2012)</i>
<i>Z-R conversion</i>	<i>30-40 (conditionally dependant on precipitation magnitude)</i>	<i>Plural Z-R relations (Zhang et al 2011)</i>
<i>Local gauge bias correction</i>	<i>10-100 (conditionally dependant on precipitation magnitude)</i>	<i>Improved distance weighting (Zhang et al. 2011)</i>

5. Practical Considerations

5.1 Numerical Computation Considerations

Endian

The WDSS-II production package assumes IEEE little-endian environment. However output data are in NetCDF format so no swapping is necessary.

Precision

The code is run in 64-bit mode.

Parallelization

This production package is considered computationally intensive and is implemented in a parallelized platform – CICS-NC computational cluster.

5.2 Programming and Procedural Considerations

The code that implements the severe weather processing (WDSS-II) requires a license specific to the platform where it is run. The code that processes the precipitation CDRs follows standard procedural programming and therefore does not require any unusual programming techniques.

5.3 Quality Assessment and Diagnostics

5.4 Exception Handling

Error and exception conditions are handled by direct checking of conditions/return codes in the main control flow rather than by a language-supported exception construct.

5.4.1 Conditions Checked

The following conditions identify errors that necessitate the program terminate. These errors are trapped and the program prints a suitable message, then exits gracefully with a non-zero status indicating the type of error.

- If an incorrect number of arguments are supplied to the program, a usage message is printed and it exits.
- If there is an error opening or reading an input file, the program prints an error message and exits.
- If there is an error creating or writing to an output file, the program prints an error message and exits.

The following exceptions are trapped and recovered from by skipping over the item that can't be processed, setting codes to track this, and continuing processing with the next item:

- If there is an error opening or reading a standalone geolocation file, the processing of this radar is skipped over, and the program execution continues.

5.4.2 Conditions Not Checked

The following possible error condition is not checked for:

- In the unlikely event that the program would run out of memory, the process would terminate unexpectedly.

5.4.3 Conditions Not Considered Exceptions

Where data fields are missing or do not satisfy quality control checks (described in Section 3.2.7), quality flags are set, and for those quality issues classified as serious the corresponding data fields are set to indicate missing data. All corrections/conversions are applied only to non-missing data, and if any processing stage identifies certain data as missing, it remains missing for all future processing stages. This is considered normal processing and not an exception condition.

5.5 Algorithm Validation

The algorithm validation has been carried out with regards to geolocation correction, scan bias correction and inter-radar calibration.

5.5.1 Geolocation Correction

Not Applicable

5.5.2 Scan Bias Correction

Not Applicable for NEXRAD

5.6 Processing Environment and Resources

Computer Hardware Computer Hardware: Linux x86_64, 132 GB memory

Operating System: Red Hat Enterprise Linux Server release 6.5 (Santiago)

Programming Language: C++

Compilers: gcc

External Libraries: NetCDF 4.1.1

Total CPU Time: about Xm per radar year

Wall Clock Time: about Xm per radar year

Temporary Storage: X GB per radar year.

6. Assumptions and Limitations

6.1 Algorithm Performance

Not applicable

6.2 Sensor Performance

NEXRAD historical sensor status is available at
<https://www.ncdc.noaa.gov/nexradinv/>

7. Future Enhancements

7.1 Enhancement 1 – Backfill of NEXRAD-Re Record

The NEXRAD Reanalysis will be continued/backfilled to 1998 using the existing or most recent version of the algorithm.

7.2 Enhancement 2 – Extension of the NEXRAD-Re Record

The NEXRAD reanalysis will be extended from 2012 to present using an updated algorithm for dual polarized NEXRAD data.

8. References

Chen, S., J. J. Gourley, Y. Hong, P. E. Kirstetter, J. Zhang, K. W. Howard, Z. L. Flamig, J. Hu, and Y. Qi, 2013: Evaluation and uncertainty estimation of NOAA/NSSL next generation national mosaic QPE (Q2) over the Continental United States. *J. Hydrometeor.*, **14**, 1308–1322. doi:[10.1175/JHM-D-12-0150.1](https://doi.org/10.1175/JHM-D-12-0150.1).

Crum, T.D., Alberty, R.L., Burgess, D.W., 1993: Recording, archiving, and using WSR-88D data, *Bulletin of the American Meteorological Society*, **74** (4), 645-653.

Cocks, S. B., S. M. Martinaitis, B. Kaney, J. Zhang, and K. Howard, 2016: MRMS QPE performance during the 2013-14 cool season. *J. Hydrometeor.*, **17**, 791–810. doi:[10.1175/JHM-D-15-0095.1](https://doi.org/10.1175/JHM-D-15-0095.1).

Cunha, L. J. Smith, M.L. Baeck, W. Krajewski, 2013: An Early Performance Evaluation of the NEXRAD Dual-Polarization Radar Rainfall Estimates for Urban Flood Applications, Weather and Forecasting, DOI: <http://dx.doi.org/10.1175/WAF-D-13-00046.1>

Fulton, R.A. 1998. WSR-88D Polar-to-HRAP Mapping, NOAA Technical Memorandum, National Weather Service, Office of Hydrology, Hydrologic Research Laboratory, Silver Spring MD, August 1998.

Grams, H. M., J. Zhang, and K. L. Elmore, 2014: Automated identification of enhanced rainfall rates using the near-storm environment for radar precipitation estimates. *J. Hydrometeor.*, **15**, 1238–1254. doi:[10.1175/JHM-D-13-042.1](https://doi.org/10.1175/JHM-D-13-042.1).

Kitzmler, D., and Coauthors, 2011: Evolving multisensor precipitation estimation methods: Their impacts on flow prediction using a distributed hydrologic model. *J. Hydrometeor.*, **12**, 1414–1431. doi:[10.1175/JHM-D-10-05038.1](https://doi.org/10.1175/JHM-D-10-05038.1).

Klazura, G.E., Imy, D.A., 1993: A description of the initial set of analysis products available from the NEXRAD WSR-88D system, *Bulletin of the American Meteorological Society*, **74** (7), 1293-1311.

Laksmanan, V. T. Smith, G. Stumpf, and K. Hondl, 2007: “ The Warning Desicsion Support System – Integrated Information,” *Weather and Forecasting*, **22** (596-612), DOI: 10.1175/WAF1009.1

Lakshmanan, V., A. Fritz, T. Smith, K Hondl, and G. J. Stumpf, 2007: An automated technique to quality control radar reflectivity data. *J. Appl. Meteor. Climatol.*, **46**, 288-305

Martinaitis, S. M., S. B. Cocks, Y. Qi., B. T. Kaney, J. Zhang, and K. Howard, 2015: Understanding winter precipitation impacts on automated gauge observations within a

real-time system. *J. Hydrometeor.*, **16**, 2345–2363. doi:[10.1175/JHM-D-15-0020.1](https://doi.org/10.1175/JHM-D-15-0020.1).

Tang, L., J. Zhang, C. Langston, J. Krause, K. Howard, and V. Lakshmanan, 2014: A physically based precipitation–nonprecipitation radar echo classifier using polarimetric and environmental data in a real-time national system. *Wea. Forecasting*, **29**, 1106–1119. doi:[10.1175/WAF-D-13-00072.1](https://doi.org/10.1175/WAF-D-13-00072.1).

Qi, Y., S. Martinaitis, J. Zhang, and S. Cocks, 2016: A real-time automated quality control of hourly rain gauge data based on multiple sensors in MRMS system. *J. Hydrometeor.*, **17**, 1675–1691. doi:[10.1175/JHM-D-15-0188.1](https://doi.org/10.1175/JHM-D-15-0188.1).

Qi, Y., J. Zhang, B. Kaney, C. Langston, and K. Howard, 2014: Improving WSR-88D radar QPE for orographic precipitation using profiler observations. *J. Hydrometeor.*, **15**, 1135–1151. doi:[10.1175/JHM-D-13-0131.1](https://doi.org/10.1175/JHM-D-13-0131.1).

Qi, Y., J. Zhang, and P. Zhang, 2013: A real-time automated convective and stratiform precipitation segregation algorithm in native radar coordinates. *Q. J. R. Meteorol. Soc.*, **139**, 2233–2240. doi:[10.1002/qj.2095](https://doi.org/10.1002/qj.2095).

Qi, Y., and J. Zhang, 2013: Correction of radar QPE errors associated with low and partially observed brightband layers. *J. Hydrometeor.*, **14**, 1933–1943. doi:[10.1175/JHM-D-13-040.1](https://doi.org/10.1175/JHM-D-13-040.1).

Vasiloff, S. V., K. W. Howard, and J. Zhang, 2009: Difficulties with correcting radar rainfall estimates based on rain gauge data: A case study of severe weather in Montana on 16–17 June 2007. *Wea. Forecasting*, **24**, 1334–1344. doi:[10.1175/2009WAF2222154.1](https://doi.org/10.1175/2009WAF2222154.1).

Vasiloff, S. V., and Coauthors, 2007: Improving QPE and very short term QPF: An initiative for a community-wide integrated approach. *Bull. Amer. Meteor. Soc.*, **88**, 1899–1911. doi:[10.1175/BAMS-88-12-1899](https://doi.org/10.1175/BAMS-88-12-1899).

Wu, W., D. Kitzmiller, and S. Wu, 2012: Evaluation of radar precipitation estimates from the National Mosaic and Multisensor Quantitative Precipitation Estimation System and the WSR-88D precipitation processing system over the Conterminous United States. *J. Hydrometeor.*, **13**, 1080–1093. doi:[10.1175/JHM-D-11-064.1](https://doi.org/10.1175/JHM-D-11-064.1).

Xu, X., K. Howard, and J. Zhang, 2008: An automated radar technique for the identification of tropical precipitation. *J. Hydrometeor.*, **9**, 885–902. doi:[10.1175/2007JHM954.1](https://doi.org/10.1175/2007JHM954.1).

Zhang, J., and Coauthors, 2016: Multi-Radar Multi-Sensor (MRMS) quantitative precipitation estimation: Initial operating capabilities. *Bull. Amer. Meteor. Soc.*, **97**, 621–637. doi:[10.1175/BAMS-D-00174.1](https://doi.org/10.1175/BAMS-D-00174.1).

Zhang, J., Y. Qi., C. Langston, B. Kaney, and K. Howard, 2014: A real-time algorithm for

merging radar QPEs with rain gauge observations and orographic precipitation climatology. *J. Hydrometeor.*, **15**, 1794–1809. doi:[10.1175/JHM-D-13-0163.1](https://doi.org/10.1175/JHM-D-13-0163.1).

Zhang, J., Y. Qi, K. Howard, C. Langston, and B. Kaney, 2012: Radar Quality Index (RQI) – A combined measure of beam blockage and VPR effects in a national network. *Weather Radar and Hydrology*, R. J. Moore, S. J. Cole, and A. J. Illingworth, Eds., International Association of Hydrological Science, 388–393.

Zhang, J., Y. Qi, D. Kingsmill, and K. Howard, 2012: Radar-based quantitative precipitation estimation for the cool season in complex terrain: Case studies from the NOAA Hydrometeorology Testbed. *J. Hydrometeor.*, **13**, 1836–1854. doi:[10.1175/JHM-D-11-0145.1](https://doi.org/10.1175/JHM-D-11-0145.1).

Zhang, J., and Coauthors, 2011: National Mosaic and Multi-Sensor QPE (NMQ) System: Description, results, and future plans. *Bull. Amer. Meteor. Soc.*, **92**, 1321–1338. doi:[10.1175/2011BAMS-D-11-00047.1](https://doi.org/10.1175/2011BAMS-D-11-00047.1).

Zhang, J., and Y. Qi, 2010: A real-time algorithm for the correction of brightband effects in radar-derived QPE. *J. Hydrometeor.*, **11**, 1157–1171. doi:[10.1175/2010JHM1201.1](https://doi.org/10.1175/2010JHM1201.1).

Zhang, J., C. Langston, and K. Howard, 2008: Brightband identification based on vertical profiles of reflectivity from the WSR-88D. *J. Atmos. Oceanic Technol.*, **25**, 1859–1872. doi:[10.1175/2008JTECHA1039.1](https://doi.org/10.1175/2008JTECHA1039.1).

Appendix B. NEXRAD Details

For detailed information on NEXRAD data and access see -
<https://www.ncdc.noaa.gov/data-access/radar-data/nexrad>.